



Numerical Investigation of Detonation Combustion Wave in Pulse Detonation Combustor with Ejector

P. Debnath^{1†} and K. M. Pandey²

¹ *Department of Mechanical Engineering, National Institute of Technology Agartala, Tripura, India, 799046*

² *Department of Mechanical Engineering, National Institute of Technology Silchar, Assam, India, 788010*

†*Corresponding Author Email: er.pinkunits@yahoo.com*

(Received September 30, 2016; accepted December 14, 2016)

ABSTRACT

Detonation combustion based engines are more efficient compared to conventional deflagration based engines. Pulse detonation engine is the new concept in propulsion technology for future propulsion system. In this contrast, an ejector was used to modify the detonation wave propagation structure in pulse detonation engine combustor. In this paper k- ϵ turbulence model was used for detonation wave shock pattern simulation in PDE with ejectors at Ansys 14 Fluent platform. The unsteady Euler equation was used to simulate the physics of detonation wave initiation in detonation tube. The computational simulations predicted the detonation wave flow field structure, combustion wave interactions and maximum thrust augmentation in supersonic condition with ejectors at time step of 0.034s. The ejector enhances the detonation wave velocity which reaches up to 2226 m/s in detonation tube at same time step, which is near about C-J velocity. Further the time averaged detonation wave pressure, temperature, wave velocity and vortex characteristics interaction are obtained with short duration of 0.023s and fully developed detonation wave structures are in good agreement with experimental shadowgraph, which are cited from previous experimental research work.

Keywords: Detonation; Ejector; Computational fluid dynamics; Pulse detonation engine; Thrust.

NOMENCLATURE

<i>CFD</i>	Computational Fluid Dynamics	Ma	Mach Number
<i>CEA</i>	Chemical Equilibrium and Applications	P	pressure
<i>PDE</i>	Pulse Detonation Engine	t	time
CJ	Chapman Jouguet	T	temperature
d	diameter of the ejector	ρ	density
L	length of the ejector		

1. INTRODUCTION

Ejector is a device which is placed downstream of the pulse detonation combustor exit and it's used for propulsion performance implementation. The ejector geometry at the exit of detonation tube has been drastically affected the performance of PDE, like the detonation wave initiation and acceleration in detonation tube. The detonation wave velocity has been observed to increase linearly with operating cycle time (Kailasanath, K. 2003). (Pandey, K. M. and P. Debnath, 2016) studied the "Recent Advances in Pulse Detonation Engines", in their review study, addressing the different computational and experimental analysis of pulse detonation engine and future research scope. Two-

dimensional ejector was provided to pulse detonation engine for parametric study by (Allgood, D. and E. Gutmark, 2004, January). The performance was observed in the inlet geometry and axial position relative to the exhaust section of the PDE. The rotary wave ejector concept has high significant potential for thrust augmentation relative to pulse detonation engine (Nalim, M. R., Z. A. Izzy and P. Akbari, 2012). The experimental studies were performed to investigate the ejector's effects on the performance of a pulse detonation engine. Their results indicate that thrust augmentation increases at high operating frequency (Bai Q. D. and C. S. Weng, 2014). The starting vortex generation and performance were affected by the geometry of ejectors. They also observed that the

ejector length has less important on overall performance compared to the ejector diameter (Zheng F. *et al.*, 2011).

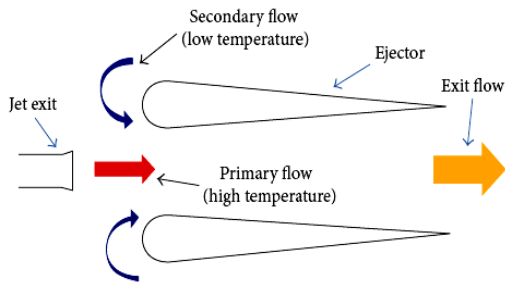


Fig. 1. Mass flow through the ejector (Zheng F. *et al.*, 2011).

The ejectors were analyzed to investigate the thrust augmentation in pulse detonation engines. The numerical results were describing the primary detonation wave propagation processes of PDE and secondary detonation wave propagation in ejector system. The details of the flow field of detonation wave propagation inside the detonation tube and injection into the ejectors were studied (Zhang H. *et al.*, 2011). The combined effect of bypass and ejector concept was analyzed in air breathing pulse detonation engine. The calculated results showed that the APDE performance was determined by shock loss induced by the throat and diameter of the nozzle (Cha X. *et al.*, 2008). The unsteady thrust augmentation was studied by Zheng F. *et al.* in 2009. The optimum starting vortex was generated by optimum diameter of the ejector and investigation was showed a minor effect of the ejector length. The linear array and compact box array of detonation tube with axisymmetric ejectors were examined (Hoke J. L. *et al.*, 2009). The secondary flow was engaged with the ejector lip by linear detonation tube. The thrust augmentation was found to increase with ejector length. The ejector performance was observed to be strongly dependent on the operating fill fraction (Allgood D. *et al.*, 2008). The thrust augmentation as a function of ejector entrance to detonation tube exit distance showed the two maxima. The thrust augmentation of 2.5 was observed using a tapered ejector. The thrust augmentation depends on the distance between the detonation tube exit and the ejector entrance. The maximum thrust depends on both positive and negative values of this distance (Wilson J. *et al.*, 2007). The tapered ejector and cylindrical ejector configuration were tested and compared. The highest level of thrust augmentation was achieved in tapered ejector configuration (Paxson D. E., *et al.*, 2006). The experimental studies were employed an H₂-air pulse detonation engine to improve the operation of ejector augmenters driven. In this research, straight and diverging ejectors were investigated (Glaser, A. J. *et al.*, 2008). Again in 2011, Changxin P. *et al.* experimentally studied to improve the performance of ejector driven by an air-breathing pulse detonation engine with convergent nozzle at different operating frequencies. The maximum thrust augmentation was obtained in single ejector

with L/D=2. The effect of blockage ratio on deflagration to detonation transition in detonation tube has been simulated using computational fluid dynamics by Debnath P. and K. M. Pandey in 2014. In this simulation, it was found that lesser the blockage ratio, faster would be the deflagration flame. Further, in 2016, Debnath P. and K. M. Pandey, computationally studied the thermal exergy as well as efficiency of exergy for hydrogen-air detonation in pulse detonation engine due to combustor fuel, from economic point of view. The computational fluid dynamics analysis was carried out, utilizing three hydrogen mass fractions of 0.25, 0.35 and 0.55 respectively in combustion process.

The simulated results show that exergy loss in the deflagration combustion process is higher in comparison to the detonation combustion process. Higher efficiency of exergy was also observed in lesser fuel mass fraction. The CFD based combustion simulation in confined swirling flame burner has been studied (Klancisar M., *et al.*, 2016). The mixing field intensity in turbulent flow, combustion heat release rate, chemical kinetics were studied in these simulations and CFD result showed that it is ecological acceptable for industrial burner.

The current research work was carried out to analyze the effects of ejectors for the detonation wave flow patterns in detonation tube at different operating cycle time and gaseous hydrogen fuel was used as a combustible fuel. Also, the shortest possible time for fully developed detonation wave was evaluated.

2. NUMERICAL METHODOLOGY

2.1. Governing Equations

The three dimensional, time-dependent compressible ($M > 2$) Euler equations with chemical reaction terms in detonation tube coordinates are used as governing equations:

$$H = \frac{\partial U}{\partial t} + \frac{\partial E}{\partial \xi} + \frac{\partial F}{\partial \eta} + \frac{\partial G}{\partial \zeta} \quad (1)$$

Where, U is the vector of conserved variables, E, F and G are the convective flux vectors and source vectors H are defined as the following:

$$U \equiv \begin{pmatrix} \rho \\ \rho u \\ \rho v \\ \rho w \\ e \\ \rho \beta \end{pmatrix}; \quad E \equiv \begin{pmatrix} \rho \bar{U} \\ \rho \bar{U} u + p \zeta_x \\ \rho \bar{U} v + p \zeta_y \\ \rho \bar{U} w + p \zeta_z \\ \bar{U} (p + e) \\ \rho \bar{U} \beta \end{pmatrix}; \quad F \equiv \begin{pmatrix} \rho \bar{V} \\ \rho \bar{V} u + p \eta_x \\ \rho \bar{V} v + p \eta_y \\ \rho \bar{V} w + p \eta_z \\ \bar{V} (p + e) \\ \rho \bar{V} \beta \end{pmatrix};$$

$$G \equiv \begin{pmatrix} \rho \bar{W} \\ \rho \bar{W} u + p \zeta_x \\ \rho \bar{W} v + p \zeta_y \\ \rho \bar{W} w + p \zeta_z \\ \bar{W} (p + e) \\ \rho \bar{W} \beta \end{pmatrix}; \quad S \equiv \begin{pmatrix} 0 \\ 0 \\ 0 \\ 0 \\ 0 \\ \rho \dot{\omega} \beta \end{pmatrix} \quad (2)$$

Where,

$$\bar{U} = u \xi_x + v \xi_y + w \xi_z$$

$$\bar{V} = u \eta_x + v \eta_y + w \eta_z$$

$$\bar{W} = u \zeta_x + v \zeta_y + w \zeta_z \quad (3)$$

To solve the above Euler equations of reacting flows the conservation equations can be split into the following equations:

$$\frac{\partial U}{\partial t} + \frac{\partial E}{\partial \xi} = 0 \quad (4)$$

$$\frac{\partial U}{\partial t} + \frac{\partial F}{\partial \eta} = 0 \quad (5)$$

$$\frac{\partial U}{\partial t} + \frac{\partial G}{\partial \zeta} = 0 \quad (6)$$

In these systems of equations the density ρ (M, t) is the total density of the whole gas in position M and at time t.

The ρ is calculated as sum of mass fraction (Y_i) and density (ρ_i) of each species,

$$\rho = \sum_i^n Y_i \rho_i \quad (7)$$

Where, $i=1$ to n^{th} species

The following equations of state are also defined as given below

$$Y_n = 1 - \sum_{i=1}^{n-1} Y_i \quad (8)$$

$$P = \rho RT \sum_{i=1}^n \frac{Y_i}{M_n} \quad (9)$$

Where, β stands for reaction parameter, $\dot{\omega}_\beta$ stands for reaction rate, which follow the Arrhenius law, T is the temperature.

2.2. Computational Domain Discretization

The continuity equation, the Euler equation for chemical reaction for combustible mixture and realizable k- ϵ turbulence model are numerically solved by the commercial software Ansys 14 Fluent with finite volume method for discretizing the differential equation and computing detonation wave flow structure. The computational domain was discretized into a finite number of elementary control volumes. The Semi-Implicit Method for Pressure-Linked Equation (SIMPLE) was used for solving the scalar variables with the k- ϵ turbulence model.

2.3. Mathematical Formulation

In this present study, the Finite Volume Method is used to solve the conservation equations of the turbulent combustion in PDE combustor, which allows calculating the PDE thrust. Among these conservation equations, there is one mass balance equation. The Eq. (10) represents the mass balance

with indicial notation, where ρ is the density, \bar{V} is the velocity vector and value of \bar{S}_m is zero for steady-state flow.

$$\frac{\partial \rho}{\partial t} + \nabla \cdot (\rho \bar{V}) = \bar{S}_m = 0 \quad (10)$$

The momentum equation must be solved along with the mass balance equation. The Eq. (11) represents the momentum equation, where, $\bar{\tau}$ is the stress tensor (described below), and $\rho \bar{g}$ and \bar{F} are the gravitational body force and external body forces (e.g., that arise from interaction with the dispersed phase), respectively.

$$\frac{\partial}{\partial t} (\rho \bar{V}) + \nabla \cdot (\rho \bar{V} \bar{V}) = -\nabla p + \nabla \cdot \bar{\tau} + \rho \bar{g} + \bar{F} \quad (11)$$

The stress tensor is given by

$$\bar{\tau} = \mu \left[(\nabla \cdot \bar{V} + \nabla \cdot \bar{V}^T) - \frac{2}{3} \nabla \cdot \bar{V} I \right] \quad (12)$$

Where μ is the molecular viscosity, I is the unit tensor, and the second term on the right hand side is the effect of volume dilation.

2.4. Turbulence Model

The realizable k- ϵ turbulence model provides superior performance for flows involving rotation, boundary layers under strong adverse pressure gradients, separation, and recirculation. The modeled transport equations for k and ϵ in the realizable k- ϵ model are:

$$\frac{\partial (\rho k)}{\partial t} + \frac{\partial (\rho k u_j)}{\partial x_j} = \frac{\partial}{\partial x_j} \left[\left(\mu + \frac{\mu_t}{\sigma_k} \right) \frac{\partial k}{\partial x_j} \right] + G_k + G_b - \rho \epsilon - Y_M + S_k \quad (13)$$

And

$$\frac{\partial (\rho \epsilon)}{\partial t} + \frac{\partial (\rho \epsilon u_i)}{\partial x_i} = \frac{\partial}{\partial x_j} \left[\left(\mu + \frac{\mu_t}{\sigma_\epsilon} \right) \frac{\partial \epsilon}{\partial x_j} \right] + \rho C_1 S_\epsilon - \rho C_2 \frac{\epsilon^2}{K + \sqrt{v \epsilon}} + C_{1\epsilon} \frac{\epsilon}{K} C_{3\epsilon} G_b + S_\epsilon \quad (14)$$

Where,

$$C_1 = \max \left[0.43, \frac{\eta}{\eta + S} \right], \quad \eta = S \frac{K}{\epsilon} \quad \text{and} \quad S = \sqrt{2 S_{ij} S_{ij}}$$

In these equations, G_k represents the generation of turbulence kinetic energy due to the mean velocity gradients. G_b is the generation of turbulence kinetic energy due to buoyancy. Y_M represents the contribution of the fluctuating dilatation in compressible turbulence to the overall dissipation rate. C_2 and $C_{1\epsilon}$ are constants. σ_k and σ_ϵ are the turbulent Prandtl numbers for k and ϵ , respectively. S_k and S_ϵ are user-defined source terms.

3. MATERIALS AND METHOD

Physical Model of PDE with Ejectors

The parametric relation of physical model of pulse detonation engine in case of ejector geometry design is shown in Fig. 2. For the present study, the following geometry dimension relation was used as the base of physical model dimension design. The ejector dimension relations for the physical model are $\frac{D}{d} = 2.4$, $\frac{\delta}{d} = 2$, $\frac{L}{d} = 8.6$, $\frac{r}{d} = 0.6$ and taper angle is $\alpha = 4^\circ$. Where, δ is the distance between the ejector nose and the exit of the PDE and d is the diameter of the ejector at the smallest position. The pulse detonation engine combustor consists of a straight cylindrical detonation tube with length of 60 cm. The combustion chamber is composed of a convergent nozzle having a length of 10.5 cm. The length of exit divergent nozzle of PDE is 4.5 cm. The dimensions of ejectors are calculated considering the above parameter relations. The pulse detonation engine was a single tube with 60 cm inner diameter and total length of 82.5 cm as shown in Fig. 3. The diameters of the nozzle at the throat and the exit planes are 8.17 mm and 12 mm, respectively. The ejector geometry configuration is chosen from the dimension relation of experimental set up of (Zheng F. *et al.*, 2011). The computational domains are used for unsteady simulations for complete configuration of PDE with ejectors. The detonation wave was initiating from the upstream end of the injector passages and extending through the combustor than terminating just downstream of the choked nozzle throat.

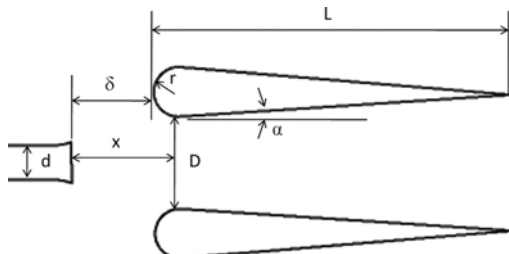


Fig. 2. Geometrical parameters relation of the ejector [Zheng F. *et al.*, 2011].

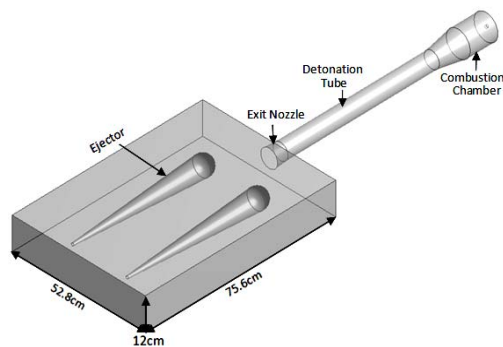


Fig. 3. Three dimensional physical model of ejectors at end of the divergent pulse detonation engine.

4. COMPUTATIONAL METHODOLOGY

The commercially available CFD package Fluent 14 solver is used to simulate the ejector effect on pulse detonation engine combustion process. The ejector effect on the combustion wave flow field inside the detonation tube as well as PDE combustor was simulated using aforesaid CFD code.

4.1. Grid Generation and Refinement Test

The meshes of computational domains are used for the computational simulations which are shown in Fig. 4. The elements of computational domains have been generated by Tet/Hybrid type mesh. The accurate computational result depends on grid resolution. The refinement of grid resolutions is used, where the grid resolution dominates the accurate computational results. The grid refinement tests of computational domains are presented in Table 1. Here the detonation wave velocities are considered for grid independence test. Fig. 5 represents the variation of detonation wave velocities with variation of number of nodes of computational domain. The successful total number of nodes and elements are found to be 414711 and 2289337, from grid independence test.

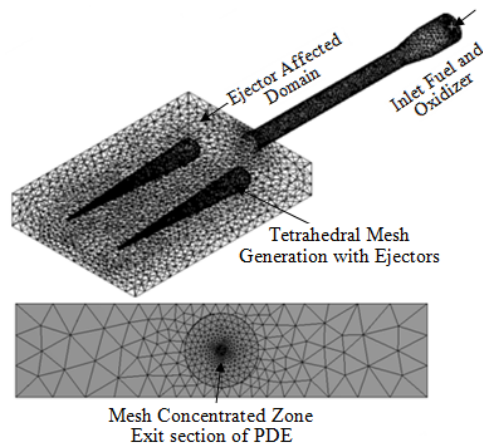


Fig. 4. Tetrahedral mesh generation of divergent PDE with ejectors.

Table 1 Mesh refinement level of computational domain with ejectors

Grid Refinement Level	Number of Nodes	Number of Elements
1	156531	837914
2	213046	1159445
3	252263	1375261
4	319076	1752011
5	414711	2289337
6	532182	2628129

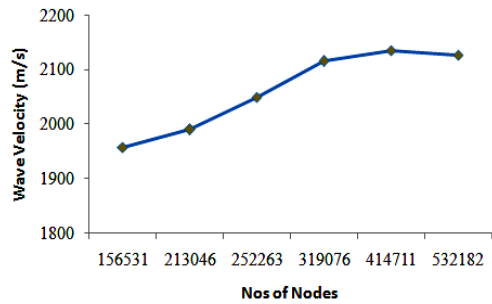


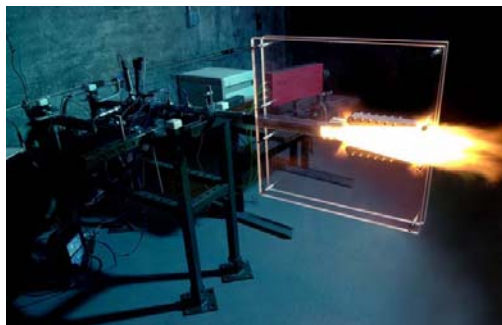
Fig. 5. Grid independence test for computational domain with ejectors.

4.2. Boundary Conditions for Computational Simulation

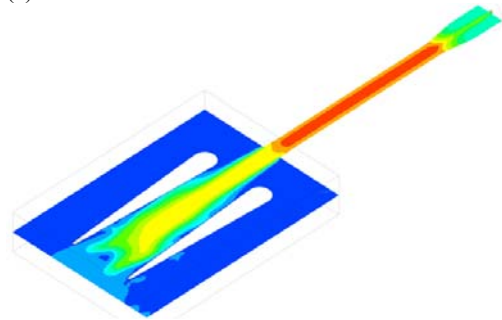
The standard k-ε turbulence model is used for computational simulations. The air inlet Mach number is $Ma=1.319$ and inlet simulations of hydrogen-air mixture temperatures are 298 K and 787 K. Species mass fraction of incoming air contains $H_2=0.000005$, $O_2=0.2035$ and $H_2O=0.0303$. Inlet fuel having Mach number is $Ma=1.784$ and the initial combustion temperature is 298 K, species mass fraction of H_2 utilization is 1.5%.

5. RESULTS AND DISCUSSIONS

Four detonation wave flow structures were numerically simulated and flow fields were investigated for different cycle time. Fully developed detonation wave was observed from contour plot analysis.



(a)



(b)

Fig. 6 (a) Photographs of UC PDE with ejectors while firing (Glaser A. J., 2007) and (b) present CFD post contour plot of combustion wave velocity (m/s).

5.1. CFD Work Validation with Experimental Shadowgraph

The computational simulations of effects of ejectors on pulse detonation engine propulsion system are theoretically sound, but these computational simulations must be validated with experimental work. Fig. 6 (a) shows the experimental shadowgraph of UC PDE test model (Glaser A. J., 2007) and Fig. 6(b) shows the present contour plot analysis of effect of ejectors on detonation wave velocity in detonation tube and exhaust PDE combustion products. The comparison between present CFD simulation and experiment are almost similar.

5.2. Detonation Wave Structure Analysis

The evaluation of the ejector effect on pulse detonation engine combustor is to energize the secondary flow (in ambient) with the primary flow in combustor with high temperature and combustible product flow. The velocity and pressure contour fields are particularly the interests in the flow region between the detonation tube exit and ejectors entrance area. The process of combustion flow field for the detonation wave initiation and transition to detonation wave inside the detonation tube and the effect of ejectors have been visualized based on the computational results. The coherent and induced flow pattern was generated in the tube center based on the effect of left and right side ejectors. The stronger detonation wave velocity was initiated in detonation tube. The PDE ejectors maintain high pressure level after escaping the detonation wave product from detonation tube. The detonation wave characteristics and reacting shock flow patterns are affected by ejectors. When the detonation wave reaches the open end of the detonation tube, the combustion products expand in front of the ejectors. A diffracted shock and a reflected detonation wave are created. The combustion chamber pressure is above the atmospheric pressure and it generates the propulsion thrust. The pressure variation takes place at the exit of the detonation tube and entrance of the ejectors. From cited literature review the detonation wave velocities of 1428.6 m/s, 1254.7 m/s, 1295.3 m/s and 1250.5 m/s were located between different transducer points with the frequencies of 8, 10, 12 and 15 Hz (Wilson J. *et al.*, 2007 and Paxson D. E. *et al.*, 2006) and their experimental results were compared with the C-J gaseous detonation wave characteristics of gasoline-air mixture, which was calculated by Chemical Equilibrium and Applications (CEA) code. The effect of detonation wave velocity was investigated from contour plot analysis as shown in Fig. 7. By changing the cycle time alone, the detonation wave speed of 890.4 m/s at a time of 0.02s and a maximum velocity of 2226 m/s at 0.033s were obtained. The contour plot of the detonation wave velocity of 0.33s detonation blow down showed a completely detached shock exiting the tube. The key parameters of detonation wave structures are formed during the blow down process. As such, it was found that leading shock wave, starting vortex and Mach disk appeared at the

end of the detonation tube. From the contour plot-analysis, it was found that detonation wave velocity has magnitudes of 890.4 m/s, 2003 m/s, 2126 m/s and 2226 m/s in time interval of 0.02s, 0.023s, 0.033s and 0.034s. The detonation wave velocity as well as pressure, temperature gradually reached to C-J level with increasing the operating time. The time stepping contour plot-simulation clearly shows that after 0.033s cycle operating time, detonation wave velocity changes no more. So, time $t=0.033s$ is the minimum cycle time required to reach the fully developed detonation wave. The detonation wave speed also depends on the fuel and oxidizer used in combustor as well as on the gas initial conditions (pressure and to a lesser extent temperature) and stoichiometric ratio.

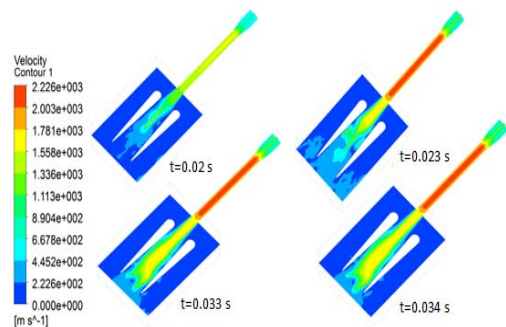
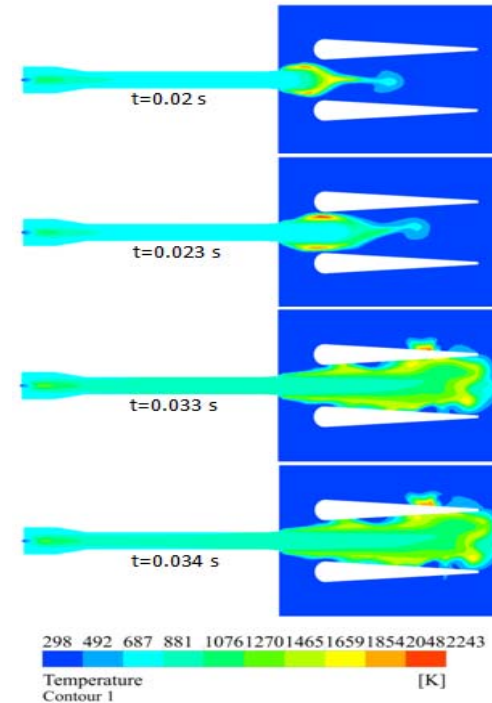


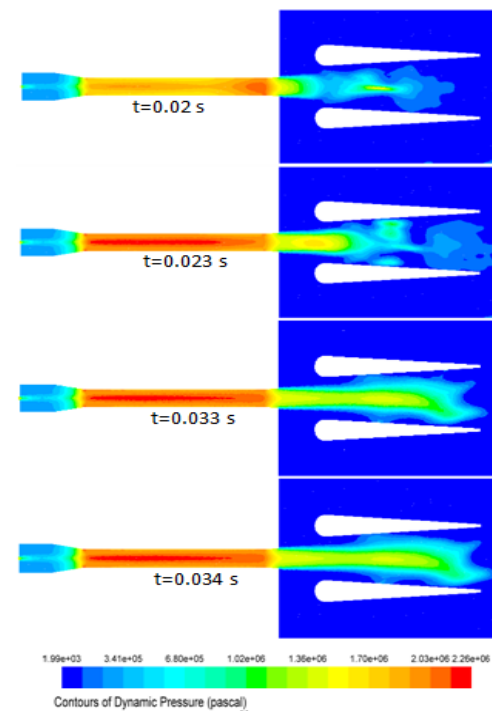
Fig. 7. Contour plots analysis of ejectors effect on fully developed detonation wave velocity (m/s).

Figure 8 shows the contour plots analysis of detonation wave temperature and dynamic pressure followed by the combustion of hydrogen-air mixture, which are affected by ejectors. The detonation wave propagation was found towards the ejectors. The temperature propagation contour was found at different cycle time due to effect of ejectors in detonation tube as shown in Fig. 8(a). The pressure of the detonation wave front in detonation tube coupling with deflagration wave front has been affected by ejectors. The maximum temperature was located in between two ejectors. The detonation wave temperature would increase from 1270 K to 2243 K at time step of 0.02s to 0.034s, which would increase the thermodynamics performance of PDE. The vortex ring was generated at the end of the detonation tube and in between the two ejectors as shown in Fig. 8(a). From the dynamic pressure contour plot analysis, it was found that the pressure magnitude at the exit of detonation tube is always changing with time. Large pressure difference was formed inside the detonation tube. Rapid expansion of detonation wave was formed and propulsion performance was affected by it. The combustion wave flow dynamics of the blow down process described many aspects of PDE operation. The pressure rise associated with the leading shock wave dominates in the combustion chamber and detonation tube acoustic field. In a PDE-driven ejector system, proper interaction of the toroidal vortex ring with the ejector inlet is critical to

provide maximum thrust augmentation of PDE. The simulated pressures are oscillating in detonation tube and reached up to desired Chapman Jouguet detonation wave pressure at time of 0.023s with the pressure magnitude of 22.6×10^5 Pascal as shown in Fig. 8(b).

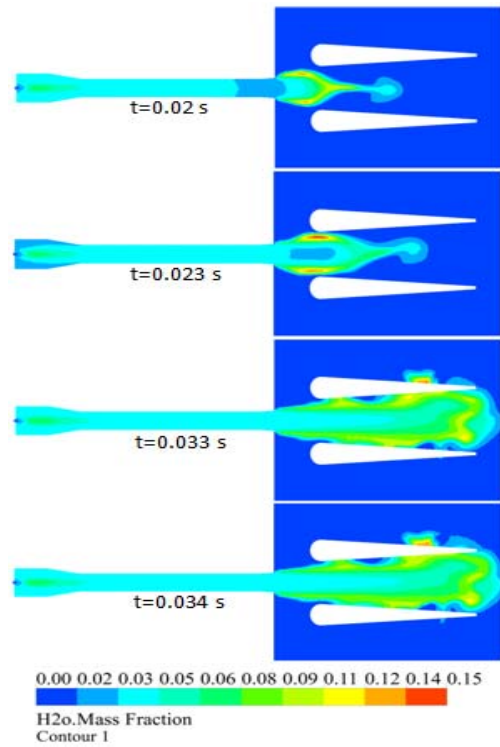


(a)

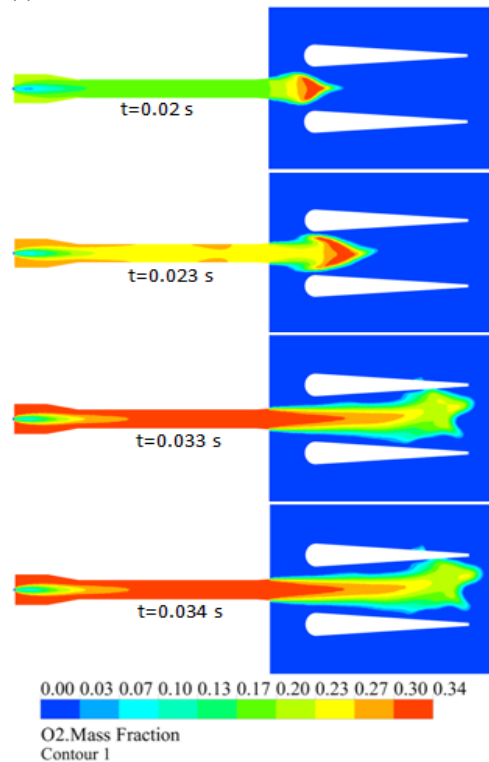


(b)

Fig. 8. Contour plots analysis of ejector effect on (a) temperature and (b) dynamics pressure of combustion wave at different time steps.



(a)



(b)

Fig. 9. Contour plots analysis of ejector effect on (a) water vapor and (b) oxygen mass fraction of combustion products at different time steps.

The contour plots analysis of ejector effect on water vapor and oxygen mass fraction of combustion products at different time steps is shown in Fig. 9. The water vapor and oxygen mass fraction contour field are particularly the interests in the flow field

region between the detonation tube exit and ejector entrance. The diffraction shocks collide in front of the ejector walls and undergo regular reflection wave. As the effective wedge angle between shock and the ejector reduces, the reflection type transitions convert to Mach reflections, indicated by the presence of the Mach stem. The vortex ring of detonation wave was just initiated in front of the ejectors and vortex cores travelled towards the channel exit and vortex ring was gradually destroyed at end of the ejectors with increasing the time steps. The vortex ring was generated at the detonation tube exit and travelled downstream toward the ejectors. The water vapor mass fraction contour plots are represented in Fig. 9(a). Figure 9(b) represents the contour plots of oxygen mass fraction which is affected by an ejector at the end of the detonation tube. The combustion products continue to move toward the exit of the ejectors. The interaction between the combustion products and vortex cores leads to the demise of vortices and filling of the ejectors section with combustion product.

5.3. Performance Analysis

5.3.1. Pressure Distribution along the Combustor

The detonation wave pressure distribution along the detonation tube and entrance of the ejectors-sections is shown in Fig. 10. The pressure variation was found in time step of 0.02, 0.023, 0.033 and 0.034 s. There is no change in pressure in between the distance of 0.0525 and 0.1425 m. Later, it was observed that $t=0.034$ s detonation wave pressure is increased up to the end of the ejector section. Detonation pressure increases with increasing the time step.

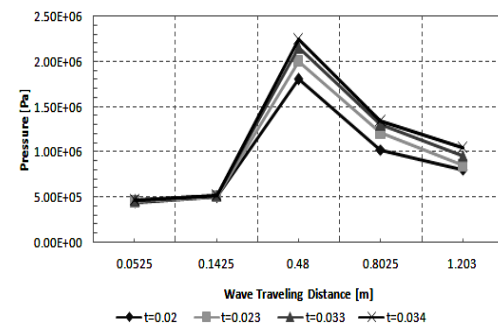


Fig. 10. Pressure distribution along the different time [s] at different wave travelling distance.

5.3.2. Thrust Analysis

The thrust is computed in PDE with ejectors by assuming an isentropic expansion of the combustible gas to atmospheric pressure. Neglecting the incoming flow velocity compared with the exhaust flow velocity, the ideal thrust of PDE is calculated by the following Eq. (15).

$$F = \dot{m}_{exit} \sqrt{2c_p T_{t-wee} \left[1 - \left(\frac{p_a}{p_{t-wee}} \right)^{\frac{\gamma-1}{\gamma}} \right]} \quad (15)$$

Where subscript “a” indicates the ambient-state which sets the nozzle discharge static pressure and “wee” indicates the wave ejector exit state supplying the nozzle. Subscript “t” stands for stagnation condition. It should be noted that this thrust is not the same as that calculated from a simple pressure and momentum balance on the detonation tube. Fig. 11 shows the thrust augmentation in PDE with ejectors. The thrust of PDE with ejectors gradually increased with operation time. The maximum thrust of PDE was obtained at $t=0.034s$ with a magnitude of 36.82N.

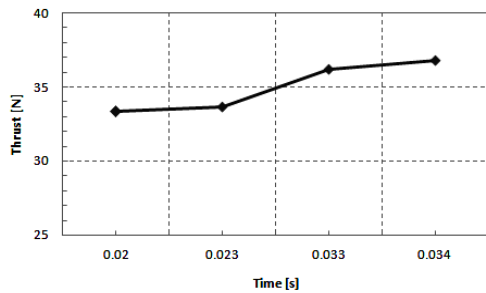


Fig. 11. Thrust augmentation of PDE with ejector.

6. CONCLUSIONS

The computational simulations revealed that the unsteady detonation wave propagation in detonation tube was affected due to the presence of ejectors at the end of the detonation tube. The simulations have shown that the pulse detonation engine with ejector produces more reliable and repeatable detonation wave. The contour plots analysis showed that the detonation wave initiated within short duration in detonation tube for the effect of ejectors at the end of the detonation tube. Another effect of ejectors was observed. The starting vortex of detonation wave propagation regime was generated in between the end of the detonation tube and the entrance of the ejectors.

- The ejector enhanced the fully developed detonation wave within short duration of $t=0.033s$.
- From contour plots-analysis, it was observed that ejectors performance is closely related to the characteristics of the vortex generated in between detonation tube exit and entrance of the two ejectors.
- From the contour plot analysis, it was observed that the detonation wave contour plots qualitatively and quantitatively agree with experimental shadow graph cited from literature.
- The strong detonation wave velocity of 2226 m/s was found in detonation tube at 0.033s, which is close to the Chapman-Jouguet detonation wave velocity.
- The strong detonation pressure magnitude was located at 0.48 m wave travelling distance at

time step of $t=0.034s$. The thrust is related to the strong detonation wave pressure and maximum thrust of 36.82N was obtained at same time duration.

REFERENCES

- Allgood, D. and E. Gutmark (2004, January). Experimental investigation of a pulse detonation engine with a 2d ejector. In *Proceeding of 42nd AIAA Aerospace Sciences Meeting and Exhibit, Reno, Nevada, AIAA-2004-864*.
- Allgood D., E. Gutmark, J. Hoke, R. Bradley and F. Schauer (2008). Performance studies of pulse detonation engine ejectors, *Journal of Propulsion and Power* 24(6). 1317-1323.
- Bai Q. D. and C. S. Weng (2014). Experimental study of ejector's effect on the performance of pulse detonation rocket engine. *Applied Mechanics and Materials* 628, 293-298.
- Cha X., Y. Chuan-jun and Q. Hua (2008). Analysis of an air-breathing pulse detonation engine with bypass and ejector. *International Journal of Turbo and Jet-Engines* 25(2).
- Changxin P., F. Wei, Z. Qun, Y. Cheng, C. Wenjuan and Y. Chuanjun, (2011) Experimental study of an air-breathing pulse detonation engine ejector. *Experimental Thermal and Fluid Science* 35, 971-977.
- Debnath P and K. M. Pandey (2016) Exergetic efficiency analysis of hydrogen-air detonation in pulse detonation combustor using computational fluid dynamics. *International Journal of Spray and Combustion Dynamics*.
- Debnath P. and K. M. Pandey (2014). Effect of blockage ratio on detonation flame acceleration in pulse detonation combustor using CFD. *Applied Mechanics and Materials* 656, 64-71.
- Glaser A. J. (2007). *Performance and Environmental Impact Assessment of Pulse Detonation Based Engine Systems*. Ph. D. thesis, Division of Research and Advanced Studies of the University of Cincinnati, Department of Aerospace Engineering.
- Glaser, A. J., N. Caldwell, E. Gutmark, J. Hoke, R. Bradley and F. Schauer (2008) Study on the operation of pulse-detonation engine-driven ejectors. *Journal of Propulsion and Power* 24(6), 1324-1331.
- Hoke, J. L., A. G Naples, L. P. Goss and F. R Schauer (2009). Schlieren imaging of a single-ejector multi-tube pulsed detonation engine. In *Proceeding of 47th AIAA Aerospace Sciences Meeting Including the New Horizons Forum and Aerospace Exposition 5-8 January, Orlando, Florida*.
- Kailasanath, K. (2003). Recent developments in the research on pulse detonation engines. *AIAA*

- Journal* 41(2), 145–159.
- Klancisar, M., T. Schloen, M. Hribersek and N. Samec (2016). Analysis of the effect of the swirl flow intensity on combustion characteristics in liquid fuel powered confined swirling flames. *Journal of Applied Fluid Mechanics* 9(5), 2359-2367.
- Nalim, M. R., Z. A. Izzy and P. Akbari (2012). Rotary wave-ejector enhanced pulse detonation engine. *Shock Waves* 22(1), 23-38.
- Pandey, K. M. and P. Debnath (2016). Reviews on recent advances in pulse detonation engines. *Journal of Combustion*.
- Paxson, D. E., P. J. Litke, F. R. Schauer, R. P. Bradley and J. L. Hoke (2006, January). Performance assessment of a large scale pulsejet-driven ejector system. In *Proceeding of 44th AIAA Aerospace Sciences Meeting and Exhibit*, Reno, Nevada.
- Wilson, J., A. Sgondea, D. E. Paxson and B. N. Rosenthal (2007). Parametric investigation of thrust augmentation by ejectors on a pulse detonation tube. *Journal of Propulsion and Power* 23(1), 108-115.
- Zhang, H., Z. Chen, X. Sun, X. Jiang and B. Li. (2011). Numerical investigations on the thrust augmentation mechanisms of ejectors driven by pulse detonation engines. *Combustion Science and Technology* 183(10), 1069-1082.
- Zheng, F., A. V. Kuznetsov, W. L. Roberts and D. E. Paxson. (2011). Influence of geometry on starting vortex and ejector performance. *Journal of Fluids Engineering*, 133(5), 1-8.
- Zheng, F., A. V. Kuznetsov, W. L. Roberts and D. E. Paxson (2009, August). Numerical study of a pulsejet-driven ejector. In *Proceeding 45th AIAA/ASME/SAE/ASEE Joint Propulsion Conference & Exhibit*, Denver, Colorado.